Translocation dynamics of freely jointed Lennard-Jones chains into adsorbing pores

Christopher J. Rasmussen, Aleksey Vishnyakov, and Alexander V. Neimark[a)]
Department of Chemical and Biochemical Engineering, Rutgers, The State University of New Jersey, 98 Brett Road, Piscataway, New Jersey 08854, USA

(Received 2 August 2012; accepted 7 September 2012; published online 9 October 2012)

Polymer translocation into adsorbing nanopores is studied by using the Fokker-Planck equation of chain diffusion along the energy landscape calculated with Monte Carlo simulations using the incremental gauge cell method. The free energy profile of a translocating chain was found by combining two independent sub-chains, one free but tethered to a hard wall, and the other tethered inside an adsorbing pore. Translocation dynamics were revealed by application of the Fokker-Planck equation for normal diffusion. Adsorption of polymer chains into nanopores involves a competition of attractive adsorption and repulsive steric hindrance contributions to the free energy. Translocation times fell into two regimes depending on the strength of the adsorbing pore. In addition, we found a non-monotonic dependence of translocation times with increasing adsorption strength, with sharp peak associated with local free energy minima along the translocation coordinate. © *2012 American Institute of Physics*. [http://dx.doi.org/10.1063/1.4754632]

I. INTRODUCTION

Polymer translocation is the process of chain movement from one compartment to another through a narrow opening that is significantly smaller than the chain itself.[1] Translocation is implicated in many physical phenomena of scientific interest, including diffusion of DNA out of the cell nucleus,[2] injection of viral genetic material into a host cell,[3] transport of proteins and polypeptides across openings,[4] and drug delivery.[5] Recent interest in computational translocation studies has been fueled partly by the desire for fast and accurate nucleotide sequencing using biological and solid-state membrane nanopores.[6] Translocation may also be an important mechanism in chromatography of macromolecules. Nanoporous adsorbents are widely employed for separation of synthetic and biological polymers.[7]

Translocation has been a classic problem in polymer physics for some time. Polymer translocation can be either unforced or forced. Unforced translocation is due to diffusion of constituent monomers through the opening. An entropic barrier that is associated with the reduction of chain conformations as the polymer threads the opening must be overcome for translocation to be successful. Forced translocation is facilitated by applied driving forces, such as electrostatic,[8] hydrodynamic,[9] or adsorption fields.[10–13] The existence of free energy barriers makes the translocation problem reminiscent to the classical problem of nucleation that is solved employing the Fokker-Plank (FP) formalism.[1,14] The pioneering works of Park and Sung[10,15] utilized the Gaussian chain model to obtain the free energy landscape during the translocation of ideal chains permeating a pore within a non-interacting membrane. It was assumed that the free energy landscape could be parameterized by the single coordinate, the degree of translocation defined as the number of monomers that have successfully translocated from one side of the membrane to the other. The translocation dynamics was modeled by the FP equation, more specifically, by the 1D Smoluchowski equation of diffusion along this coordinate, with the free energy gradient acting as a driving or resisting force depending on its sign. Muthukumar[14] has combined the FP approach with the scaling theory for the free energy landscape of translocating chains. The primary assumption of the FP approach is that translocation proceeds significantly slower than the relaxation time of the chain on either side of the membrane. Although this has been questioned using scaling arguments,[16] the approach captures the essential physics of the translocation process and the main results compare favorable with experiment.[1] Recently, Mirigian *et al.* found good agreement between the FP approach and detailed Langevin dynamics (LD) studies, even in complex polyelectrolyte systems.[17] Kong and Muthukumar extended the FP approach to unforced translocation of non-ideal polymers using self-consistent field theory (SCFT).[18] Several attempts to better fit the one-dimension dynamical approach to observed anomalous diffusion behavior has led to application of the fractional Fokker-Planck equation.[19] Translocation dynamics of both forced and unforced systems have been studied directly in simulations using LD,[17,20] Brownian dynamics,[21,22] molecular dynamics (MD),[23] dissipative particle dynamics,[24] and dynamical Monte Carlo (MC) techniques.[13,25,26] Such studies range from relatively simple, lattice models to large-scale MD systems modeling the translocation of DNA through biological pores.[27] These simulation studies suggest a rich variety of environments where translocation is relevant. For a recent review of these theoretical and simulation methods, see Ref. 28.

Previous studies suggest that forced translocation encompasses weak and strong regimes, with different scaling relationships.[13,14,29] A strong driving force masks entropic

a)Author to whom correspondence should be addressed. Electronic mail: aneimark@rutgers.edu.

confinement effects, thus the translocation can be a function of the applied force alone.[14] Conversely, in the weak regime, the driving force is on the same order as the entropic resistance, and the translocation times depend on both factors. A system of interest that exemplifies this interplay is translocation into an adsorbing pore. The attractive adsorption potential favors translocation, yet the chain suffers an entropic penalty due to confinement in the pore. The balance of these enthalpic and entropic free energy contributions is critical in many polymer systems, such as theta chain transitions[30] and the critical point of adsorption in polymer chromatography.[31] Adsorption effects on translocation through a membrane pore have been studied in several papers.[11,13] Recently, Yang and Neimark[12] employed the FP approach combined with the SCFT calculations of the free energy landscape for studies of translocation into adsorbing pores and performed a detailed study of the competition of surface adsorption and confinement effects in the process of translocation into a pore. This work increases the level of details from the mean field SCFT resolution to the molecular level of MC simulations. Although the MC simulation operates with entirely different and more realistic chain models, the results obtained below generally confirm the conclusions drawn from SCFT. We found a non-monotonic dependence on translocation times as a function of adsorption potential that can be divided into three regimes: weak potentials garner fast but improbable translocation, moderate potentials give slow translocation, and large potentials yield fast translocation.

In our MC simulations, we employ a freely jointed chain model with Lennard-Jones (LJ) non-bonded interactions that is standard in molecular modeling of polymers. As a reference, the ideal freely jointed chain model is used, in which the absence of non-bonded interactions allows for the monomer overlap. The MC simulation similar to SCFT enables calculations of the free energies of equilibrated states at given thermodynamic conditions and constraints. The translocation dynamics is not monitored explicitly; rather it is studied by solution of the FP equation of diffusion along the free energy landscape determined in MC simulation as a function of the degree of translocation. To calculate the free energy, we apply the incremental gauge cell (IGC) method suggested by us recently.[32] This method is based on the mesocanonical ensemble, which considers the system of interest in thermodynamic equilibrium with a finite reservoir called the gauge cell.[33] IGC "measures" the incremental chemical potential[34] (the difference of the chemical potential between an n-mer and an $(n+1)$-mer) by allowing the chain to grow or shrink by exchanging the terminal monomers of the chain with the free monomers in the gauge cell. The chain free energy represents the sum of the incremental chemical potentials. The IGC method was found[32] to be an order of magnitude more efficient than the modified Widom approach.[34] It has been used to study adsorption effects of confined polymers.[32,35]

The rest of this paper is structured as follows. In Sec. II, we describe the systems considered, the molecular model and simulation parameters, and the FP approach to translocation dynamics. Section III presents the results of free energy landscape calculations from MC simulation, and discusses its implication on translocation. Section IV details the analysis of translocation dynamics obtained from the integration of the FP equation. In Sec. V, we present our conclusions and critical analysis of the suggested approach.

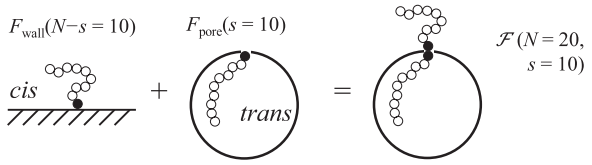

FIG. 1. Schematic of free energy calculations. Two subsystems are simulated separately – a chain tethered to a hard wall, and a chain tethered in a spherical pore. The free energy of the translocating chain (of length N, and translocation coordinate s) is the combination of the free energy of the two sub-chains. Filled circles indicate the tethered, immovable monomer.

II. MODEL

We model the translocation of a homopolymer chain into an adsorbing spherical pore (*trans* compartment) through a narrow window from a dilute solution (*cis* compartment) using off-lattice Monte Carlo simulations. The progress of the translocation process is characterized by the degree of translocation s representing the number of chain segments in the *trans* compartment. The goal of MC simulation is to determine the variation of free energy of the translocating chain $\mathcal{F}$ as a function of the degree of translocation s. The *cis* and *trans* compartments are modeled as independent subsystems (Figure 1), following the classical approach.[14,15] The *cis* compartment represents a semi-infinite space limited by the hard non-adsorbing wall, and *cis* sub-chain of length $N - s$ is considered as tethered to the wall at the pore opening, whose size is neglected. The *trans* compartment represents a spherical pore of radius R with adsorbing walls, and *trans* sub-chain of length s is tethered to the pore wall at the pore opening. The initial condition is chosen as the chain of length N in the *cis* compartment tethered to the pore opening. As the translocation progresses, the chain is modeled as a composite of *cis* and *trans* sub-chains tethered to the pore opening. The behavior of the chain within the pore opening is not considered, since the chain fragment in the pore is assumed to contribute a constant part into the total chain free energy. Within these assumptions, the free energy of the translocating chain is the sum of the free energies of the tethered chains in the *cis* and *trans* compartments

$$\mathcal{F}(N,\ s) = F_{\text{cis}}(N - s) + F_{\text{trans}}(s). \tag{1}$$

As such, the simulation problem is reduced to modeling and calculating the free energy of tethered chains in *cis* and *trans* compartments independently, as shown in Figure 1. Equation (1) determines the driving force for translocation, which is proportional to the gradient of $\mathcal{F}(N, s)$ with respect to the translocation coordinate and is supplied to the FP equation as the external potential.

Simulations were performed in the mesocanonical ensemble (MCMC)[33] using the incremental gauge cell method.[32] MCMC introduces a finite volume reservoir of non-bonded monomers (called the gauge cell) that exchange with

the system cell by addition and deletion of monomers at the free end of the tethered chain. Use of the gauge cell method brings about two main advantages: accurate determination of the chemical potential (and thus the free energy), and more efficient sampling of the phase space. Additionally, the gauge cell limits fluctuations that would otherwise result in phase changes characteristic to an open system with unconstrained fluctuations. As such, a continuous trajectory of metastable and labile states can be stabilized, and the free energy difference can be obtained by integrating along this trajectory.[36] For this reason, MCMC has become a useful tool for studying nucleation phenomena,[36,37] confined fluid phase behavior,[38] and adsorption deformation.[39] Chains are equilibrated with three types of MC moves: local monomer displacement, configurational bias regrow,[40] and exchange with the gauge cell. The simulation scheme consisted of 400 discarded equilibration sets and 500 averaged production sets, each of 850 000 attempted MC moves. Convergence was tested by monitoring error estimates in the chemical potential using blocked statistics[41] with a runtime algorithm.[42] A detailed description of the incremental gauge cell method is given in our recent paper.[32]

The polymer is modeled as a freely jointed chain. Sequential monomers are bonded with a harmonic potential

$$U_{\text{bond}}(r) = \begin{cases} \frac{1}{2}\kappa_{\text{b}}\,(r - r_0)^2 \;\; \text{for } 0.5 \le r \le 1.5 \\ \\ \infty, \text{ otherwise,} \end{cases} \tag{2}$$

where r is the distance between bonded monomers, r_0 is the equilibrium bond length set to σ_{MM}, and κ_{b} is the spring constant, taken as 400 ε/σ^2.[43] The excluded volume effect is modeled by setting non-bonded monomers to interact via the LJ potential with monomer-monomer parameters $\varepsilon_{\text{MM}}/k_{\text{B}}$ = 49.3 K, σ_{MM} = 0.394 nm, and no cut-off distance. In order to mimic good solvent conditions,[44] the simulations were performed at $k_{\text{B}}T/\varepsilon_{\text{MM}} = T^* = 8$, which is well above the theta transition temperature of LJ chains (of about 4 ε/k_{B}).[45] To demonstrate the effects of confinement on the chains of maximum length of 200 monomers the pore diameter was set to $2R = 10\ \sigma_{\text{MM}}$, which is approximately the radius of gyration of a free chain of the maximum length considered in this work. To restrict the chain's conformations in the *cis* compartment, the terminal monomer was fixed at (0, 0, 0.5 σ_{MM}), and a hard wall repulsion is implemented by rejecting the moves where monomers crossed the plane $z = 0$. Adsorption in the *trans* compartment is captured using the site averaged solid-monomer LJ potential integrated over the spherical layer of adsorption centers,[46] with σ_{SM} = 0.33 nm. The interaction strength between the pore wall and the monomer units was varied as the ratio of solid-monomer and monomer-monomer interaction energies $\xi = \varepsilon_{\text{SM}}/\varepsilon_{\text{MM}}$ = 0, 0.5, 1, 1.1, 1.3, 1.6, 2.0, 2.5, and 3.0. This range covers the regions of steric repulsion, weak adsorption, and strong adsorption. At $\xi \sim 2$, the interaction parameters roughly correspond to alkane adsorption on a silica surface.[47] Because the free energy is the sum of the incremental chemical values, it is sensitive to these values for short chains. For this reason, a more detailed potential was used for short chains, n = 1–20. This potential explicitly accounts for the translocation opening in the pore wall by partially integrating over the pore spherical surface.[48] An opening of 1 σ_{MM} was created, and the terminal bead of the chain tethered a distance of 0.5 σ_{MM} from the system boundary. This potential is shown as an *xz*-plane projection in Figure 2. The value of incremental chemical potential calculated with the more detailed and simple solid-monomer potentials are asymptotically identical for $n > 10$, thus the more detailed potential implements short chain "corrections" to the free energy.

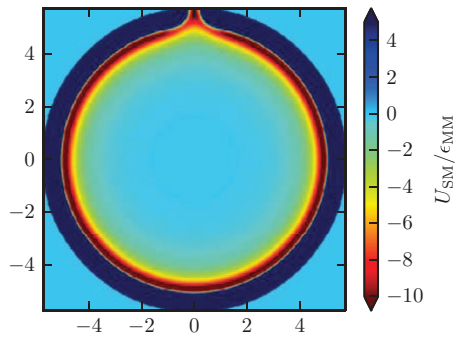

FIG. 2. Map of solid-monomer potential energy on the $y = 0$ plane, for ξ = 1.6. One end of the chain is tethered at (0, 0, $R/\sigma - 0.5$), which corresponds to the small attractive opening at the top of this plot.

Translocation dynamics are studied using the FP formalism following the approach of Park and Sung,[15] and Muthukumar,[14] as implemented in our recent theoretical work.[12] We assume that chain relaxation times are shorter than translocation times (i.e., that the *cis* and *trans* sub-chains can be considered as independent, equilibrated chains). In this case, we assume that the chain diffuses between the *cis* and *trans* compartments with the drift term proportional to the free energy gradient. The FP equation governing the translocation dynamics is

$$\frac{\partial}{\partial \tau} W(s,\tau) = \frac{\partial}{\partial s}\left[\frac{\partial \mathcal{F}(N,s)}{\partial s} W(s,\tau) + \frac{\partial}{\partial s} W(s,\tau)\right], \tag{3}$$

where $W(s, \tau)$ is the probability of a polymer chain of length N, with one initial segment in the *trans* compartment (and $N - 1$ segments in *cis* compartment) at time $\tau = 0$, to have s segments in *trans* compartment at time τ. Note that τ is the dimensionless time; it is proportional to the local friction coefficient k_0, which for a homopolymer is assumed to be independent of the degree of translocation.[15] For a complete discussion of Eq. (3), see Ref. 12.

III. RESULTS: FREE ENERGY

The incremental chemical potential, μ_{inc}, of two subsystems: a chain tethered to a hard wall and a chain tethered in a spherical adsorbing pore (Figure 1), was calculated using the IGC method.[32] The adsorption potential of the pore was varied from weak to strong interaction. The values of μ_{inc} as a function of chain length are shown in Figure 3 (top). These values were reduced by the reference state, an ideal chain with only harmonic bonds in the same system (i.e., tethered

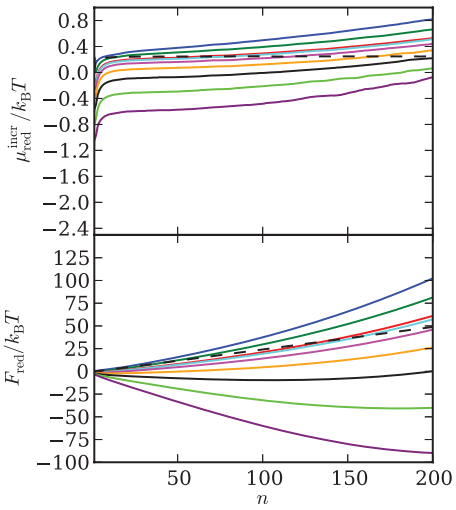

FIG. 3. (Top) The reduced incremental chemical potential of tethered chains in pores of varying adsorptive strength, as a function of chain length n. (Bottom) The reduced free energy of the same chains. Adsorptive strength is described as ξ, which is the ratio of solid-monomer LJ parameter to the monomer-monomer parameter. Solids lines indicate chains in pores with ξ = 0, 0.5, 1, 1.1, 1.3, 1.6, 2, 2.5, and 3, from most positive to most negative, respectively. Dashed lines indicate a chain tethered to a hard wall (i.e., the *cis* subsystem).

in *cis*/*trans* compartment), to better illustrate confinement effects on free energy. The dashed line indicates the hard wall *cis* sub-chain. For long chains of $n > 10$, $\mu_{\rm inc}$ is constant, as is expected for expanded coil chains well above the theta temperature.[44] The adsorption potential of was varied from $\xi = 0$ to 3.0. The incremental chemical potential of the *trans* chains rises exponentially with chain length because of increasing steric hindrance. The absolute values of $\mu_{\rm inc}$ shift to more negative values at adsorption strength increases, as favorable adsorption interactions offset the confinement entropy loss. To obtain the free energy of the tethered chain, the incremental chemical potential is summed over the chain length n.[32] The result is shown in Figure 3 (bottom). The *cis* sub-chain reduced free energy profile is increasing and linear, because of its positive and constant incremental chemical potential. The shape of the reduced free energy of the tethered chain in the adsorbing pore is more complex: depending on the adsorption potential strength, the free energy can be an increasing, decreasing, or non-monotonic (i.e., with a minimum) function of the chain length. Since the incremental chemical potentials always increase with the chain length, the minimum is due to the negative contribution from short chains. For the weak adsorption potentials up to $\xi = 0.5$, the free energy is increasing, as the respective incremental chemical potentials are all positive. As the adsorption potential increases, the free energy becomes non-monotonic: most of monomers of the short tethered chains are adsorbed at the pore wall, and the gain in enthalpy compensates for the loss of entropy. For chains shorter than 200, this regime is seen in the range of adsorption potentials 1.0–2.5. At the strongest potential of $\xi = 3.0$ considered, the free energy is still decreasing at $n = 200$, but it would achieve a minimum and then increase as the chain grows further and the pore becomes crowded with monomers. One of the important qualitative conclusions derived from these calculations is the observation that in contrast to the chains tethered to non-adsorbing hard wall, the free energy of chains confined to the adsorbing and confining pore is a nonlinear function of the chain length.

The free energy landscape of the translocating chain is calculated according to Eq. (1) as the sum of *cis*- and *trans*-sub-chain free energies shown in Figure 3. The free energy landscape of the chain with $N = 200$ total monomers is plotted as function of the degree of translocation in Figure 4. Note that the free energy terms $F_{\rm cis}$ and $F_{\rm trans}$ of Eq. (1) include the contribution from the harmonic bonds; that is, they are not the reduced values. As such, the values of $\mathcal{F}$ in Figure 4 were shifted upwards by $F_{\rm cis}(N)$ so that the depth of the free energy wells can be clearly discerned. For the weakest confinement interactions of 0 and 0.5, the free energy is positive and monotonically increases forming an uphill landscape. This suggests unfavorable conditions for translocation, which is intuitively obvious ($\xi = 0$ refers to a spherical pore with no favorable enthalpic interactions at all; a chain translocating into this pore would lose entropy and thus be unfavorable). Increasing the interaction potential to the range of 1.0–1.6, the free energy landscape becomes broader, and exhibits a minimum. Minima of $\xi = 1$ and 1.1 occur for short *trans* sub-chains ($s < 20$), while 1.3 and 1.6 have a more broad landscape, and significantly more negative minima. The minima correspond to a metastable chain configuration composed of *trans*- and *cis*- fragments, which we call a flower. In such configuration the enthalpic gain and entropic loss balance each other. As we show below, these metastable configurations represent the stall points and play an important role in translocation

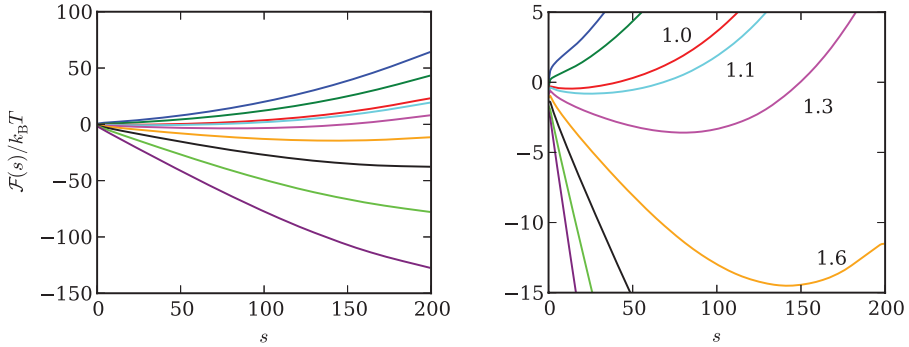

FIG. 4. (Left) The free energy landscape for an $N = 200$ chain translocating into the pore, as function of length of chain on the *trans* side s, calculated from Eq. (1). The free energy here includes the harmonic bond contribution, and is shifted by $F_{\rm cis}(N)$ for clarity. Lines correspond to ξ = 0–3 from top to bottom. (Right) Scaled to highlight free energy minima.

dynamics by significantly increasing the translocation time. Above this range ($2 \leq \xi \leq 3$), the favorable adsorption interactions are dominant and the free energy monotonically decreases forming a downhill landscape, which favors translocation, up to the length of 200 tested in our simulations. However, additional loading would begin to increase chemical potential as steric hindrance rises.

IV. RESULTS: TRANSLOCATION DYNAMICS

The dynamics of translocation was determined by numerical solution of Eq. (3). Several relevant quantities can be extracted from Eq. (3). Of particular interest is the translocation time probability distribution. The distribution of translocation times is a measurable experimental quantity, and can be interpreted to gain knowledge of the nature of translocation.[49] When using the FP formalism, it is found from the corresponding probability flux

$$P_{\text{in}}(\tau) = J|_{s=N} = -\left[k_0 \frac{\partial F(N,s)}{\partial s} W(s,\tau) + k_0 \frac{\partial}{\partial s} W(s,\tau)\right]_{s=N}, \quad (4)$$

where k_0 is the local friction coefficient. Similarly, the probability distribution of failed translocation events, when the chain comes out of the pore, is represented by the negative flux at $s = 0$. The normalized probability distributions are displayed in Figure 5. The normalizing factor is the total probability of successful translocation into the pore, given by

$$P_{\text{in}}^{\text{total}} = \int_0^\infty P_{\text{in}}(\tau)\, d\tau. \quad (5)$$

In practice, this is calculated by summation of the resulting series, multiplied by the selected $d\tau$. The lengths of the series were chosen so that final value can be approximated as zero. The first and sharpest peak is that of the strong adsorption case, $\xi = 3$, followed by 2.5. This is expected, as the strong adsorption potential forces quick translocation. However, the next two peaks are the weakest adsorption cases of $\xi = 0$ and 0.5, followed by the strong 2.0, and then by very broad distributions of the intermediate cases. This

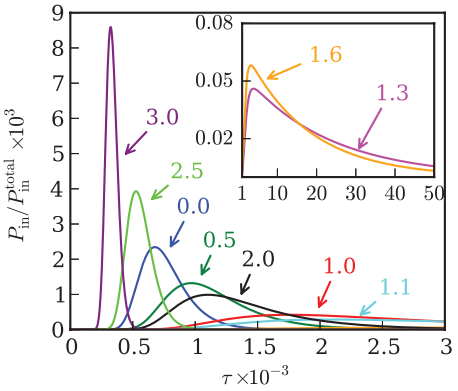

FIG. 5. The normalized probability distribution function of 200-mer chain translocating into the adsorbing pore. The inset is a magnified view of two systems: $\xi = 1.3$ and 1.6, which have extremely broad distributions.

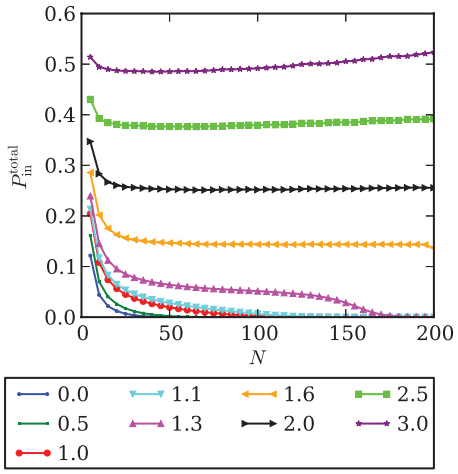

FIG. 6. The total probability of success for N-mers translocating into the adsorbing pore (Eq. (5)). Note that for long chains with unfavorable adsorption potentials, the probability tends to zero. Legend indicates adsorptive strength of spherical pore, ξ.

behavior is clearly governed by the shape of free energy profile (Figure 4). The broad distributions are the result of the minima, or stall points, found in the free energy profile. At the translocation coordinate where the minimum is found, the chain is in a metastable state, partially threaded through the translocation pore with s monomers in the adsorbing pore and N–s monomers outside. With no driving force, a successful translocation must rely on stochastic fluctuations to escape the metastable position; the time required is proportional to $\exp(-\Delta\mathcal{F}/k_{\text{B}}T)$, where here $\Delta\mathcal{F} = \mathcal{F}_{\text{min}} - \mathcal{F}(s = N)$. Thus, the deeper the free energy well, the longer the polymer will take to escape it and complete translocation. This results in the very broad time distributions for potentials where a minimum is found, namely, $\xi = 1$, 1.1, 1.3, and 1.6. Interestingly, we find that when the adsorption potential is nonexistent or very weak, successful translocation still occurs fairly quickly (the peaks of $\xi = 0$ and 0.5 are both at a smaller time than $\xi = 2$). This effect was also observed in our previous theoretical work.[12] These weak potentials both present a monotonically increasing free energy profile; translocation occurs quickly because there is no energetic advantage to slow translocation. Even though the unfavorable translocation is fast, its total probability is quite low (Figure 6). It is worth it to note that the solution to the FP equation (3) is the same for monotonically decreasing and monotonically increasing free energy, save for the prefactor.[12] This produces probability distributions of the same shape for the weak potential cases of $\xi = 0$, 0.5 and the strong potentials $\xi = 2$, 2.5, 3, albeit with a much different prefactor.

It is important to note that the distributions presented in Figure 5 are normalized by the total translocation probability (given in Eq. (5)). These values are given as a function of the length of the translocating chain for the various adsorption potentials in Figure 6. Short chains have a high probability of translocation for all potentials. Similarly, increasing adsorption potential always increases translocation probability. As the chain length increases for translocation into pores with weak or no potential, the total probability of transition approaches zero. Chains driven by intermediate adsorption

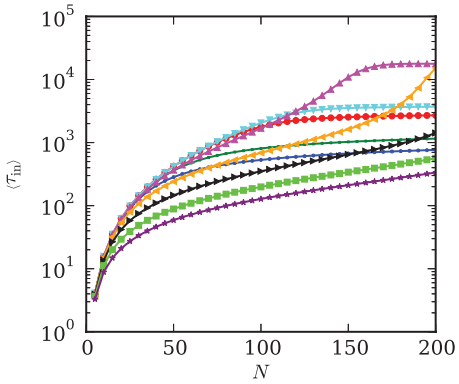

FIG. 7. Average translocation time into adsorbing pore of varying adsorption strength ξ, as function of chain length N. Refer to the legend of Figure 6.

potentials (1.6, 2) have approximately constant total probability with respect to chain length, while the strongest potentials' (2.5, 3.0) total probability increases with chain length. This effect is found when the adsorption enthalpy is the dominate contribution to the free energy, provided an excess of adsorption sites per monomer.[35] In this case, the adsorption force is strong enough that adding additional monomers (i.e., increasing the length of translocating chain) decreases the total free energy, resulting in a more likely translocation. A similar effect is found in interaction polymer chromatography, where retention increases with chain length because of increasing favorable interaction with the substrate.[50] For chains with broad time distributions at $N = 200$ (Figure 5), most have a total probability of success of zero. The exception is $\xi = 1.6$, whose overall probability of translocation is ~0.14. This suggests that broad translocation time distributions do not necessarily prevent a successful translocation event.

The most experimentally relevant property of a translocation process is the average time of successful translocation. This is given by

$$\langle\tau_{in}\rangle = \frac{\int_0^\infty \tau P_{in}(\tau)\, d\tau}{\int_0^\infty P_{in}(\tau)\, d\tau}. \quad (6)$$

The average translocation times of the LJ chain moving into an adsorbing pore are shown in Figure 7. The three regimes of adsorption strength are reflected. The strongly adsorbing pores exhibit translocation times that are exponential in nature, with a scaling exponent of ~1.37. Similarly detailed LD studies found nearly identical scaling exponents for translocation with strong forcing.[51] It is important to realize that if simulations of longer chains were performed, the scaling relation would no longer apply. For a 10 σ_{MM} diameter pore, full surface coverage is achieved with about 220 adsorbed monomers.[32] If a chain longer than this were translocating into the strongly adsorbing pore, the additional beads would experience a higher incremental chemical potential as they fill the pore volume, as they no longer directly interact with the adsorptive walls. Translocation into a weakly adsorbing pore exhibits a similar scaling behavior for the range of chain lengths tested, albeit with a smaller exponent. In addition to the faster per-monomer translocation in these weakly adsorbing systems, the prefactor is the same order as the strongly adsorbing systems. As Figure 5 also indicates, unforced chains may translocate faster than strongly forced chains. This apparent contradiction can be explained with two points: first, it is important to remember that the data presented represent the average times of *successful* translocations, and that the probability of such an event is still quite low for unforced or weakly forced systems (see Figure 6). Second, as time increases, there are significantly more chances for the chain to escape back to the lower energy *cis* state. In other words, if a successful translocation were to occur, it would have the best odds if it proceeded quickly. For the intermediate systems of $\xi = 1.3$ and 1.6, i.e., the ones exhibiting a significant free energy minimum for the $N = 200$ chain, the average translocation time shows a slow then a fast regime (as measure of translocation time per monomer scaling). The slow regime corresponds to a downhill free energy profile, akin to $\xi = 2$–3 in Figure 4. At these shorter chain lengths, there are no minima present on the free energy landscape, and translocation proceeds as with the strongly forced chains. This is followed by the fast regime plateau at larger N, representing translocation against an entropic barrier. The transition between these regimes is marked by even slower translocation times (between $N = 115$–160 for $\xi = 1.3$ and $N = 170$–200 for $\xi = 1.6$). In this range, a surmountable free energy minimum is present. In other words, the chain reached a length where a minimum is present; however, the probability of random fluctuations pushing the translocation to competition is nonzero. The chain is metastable at the minimum, and translocation times go up accordingly. The plateau in average translocation times begins were the total probability of successful translocation (Figure 6) goes to zero, and the previous "uphill" arguments apply. The two smaller values of the intermediate range ($\xi = 1$, 1.1) appear similar to the "uphill" translocations times of $\xi = 0$, 0.5, but with a larger prefactor. The minima in these two systems are relatively small, and occur at short chain length (Figure 4, right). In all cases of the "fast" translocation against a large free barrier, the probability of a successful translocation approaches zero (see Figure 6).

The non-monotonic behavior of translocation times with respect to adsorption strength is an interesting observation of this work. Figure 8 plots the average translocation time as a

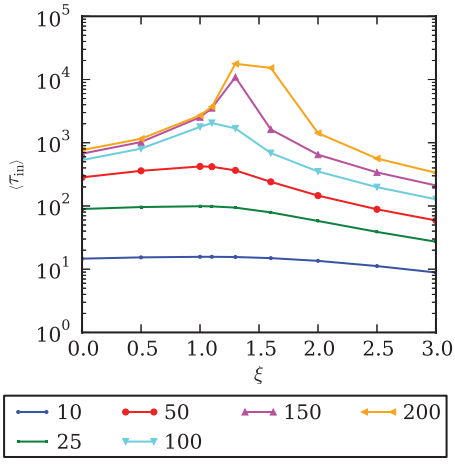

FIG. 8. Average translocation time into adsorbing pore, as function of adsorption strength for several fixed lengths N. Legend indicates chain length of translocation, N.

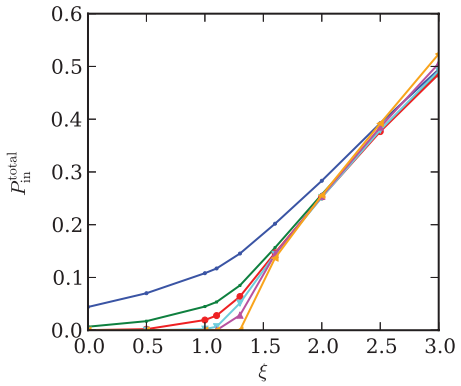

FIG. 9. The total probability of successful translocation for various chain lengths, as a function of adsorption strength.

function of adsorption strength for several lengths of chains. A prominent peak in translocation time is clear for long chains in pores in the intermediate range of potentials, where the free energy profile has a local minima corresponding to a transient metastable state. The effect is more pronounced for longer chains, since such chains must move further from the metastable state to fully translocate. Short chains are not affected because they successfully translocate before they reach the minimum. The peak arises due to the long time needed to escape the stall point at the free energy well. It falls as the adsorption potential increases, as expected. For the longest simulated chain of $N = 200$, the strongest metastable state (i.e., with the deepest free energy well along the translocation coordinate s) is found between $1.3 < \xi < 1.6$. As the chain length decreases, the position of the minima shifts to lower ξ, with $N = 150$ exhibiting a maxima near $\xi = 1.3$, and $N = 100$ at $\xi = 1.3$. The shift in the maximum for τ with changing chain length is due the additional entropic penalty from confinement of longer chains. In other words, for a given chain to reach its partially threaded metastable state, increasing length must be compensated by increasing adsorption potential. The collapse of the long chain length translocation-in times at similar values occurs where conditions are unfavorable to translocation, $\xi < 1.0$. Figure 9 shows the probability of successful translocation for the same chains as shown in Figure 8. We see that the probabilities of successful translocation into weakly adsorbing pores are mere zero for all but the shortest chains. As the likelihood of translocation begins to increase, so does the time required for successful translocation. After the adsorption potential reaches a certain strength (which depends on chain length), translocation times fall as the potential increases, as expected. This is the strong adsorption region.

V. CONCLUSIONS

We studied the dynamics of a single chain translocating into an adsorbing pore by Monte Carlo calculation of its free energy landscape using the incremental gauge cell method,[32] and application of the Fokker-Planck equation that mimics the translocation process as the diffusion along the free energy landscape. The respective free energy landscape for partially translocated chains was obtained by combining two independent *cis*- and *trans*- tethered chains. It was found that the free energy landscape of a translocating chain exhibits three characteristic behaviors: "uphill," or monotonically increasing free energy as translocation proceeds, "downhill," or decreasing free energy, and "concave" with a local minimum. This free energy minimum corresponds to a transient metastable state, where the chain comfortably balances adsorption and confinement in a flower configuration being partially adsorbed in the pore. These three energy regimes translate into very different translocation behaviors. Uphill diffusion, being unfavorable, has a very low probability of completing translocation, except for the shortest chains. However, translocation proceeds quickly if it does occur. To conceptualize this phenomenon, we can invoke a momentum analogy. One can imagine a steep hill (the energy barrier) with two climbers, one fast and one slow. The faster climber is more likely to succeed, as the slower climber has more chances to fall backwards. Downhill diffusion results in more intuitive results, with translocation times increasing with adsorption strength. This region of strong forcing was predicted quantitatively by Muthukumar.[14] The work of Krasilnikov *et al.*[52] finds experimental evidence of the non-monotonic dependence of residence times on molecular weight: they found that polyethylene glycol (PEG) residence times in an α-hemolysin pore increased with chain length, up to a molecular weight of 3000, and then decreased.

Concave translocation landscapes with free energy minima result in a very broad time distribution, up to several orders of magnitude more broad than a simple uphill or downhill case (see Figure 5, inset). When a chain that is favorably moving towards the pore reaches its free energy minimum, forward progress effectively stops as the chain fluctuates within its free energy well. At this point, successful translocation means overcoming the energy barrier from the minimum to $\mathcal{F}(s = N)$. Time for successful translocation slows accordingly. Though slow, broad translocation time distributions were found to have a non-zero probability, suggesting that addition complexities may arise in experimental systems. These phenomena highlight the importance of the interplay between enthalpy and entropy during the adsorption of polymers.

Recently, the validity of the FP method (and its assumptions) has been questioned.[16,22,26] The main concern is the result that unforced FP translocation scales as N^2, the same as (or less than) the Rouse time (the characteristic time for a free ideal chain to diffuse a distance of the order of its radius of gyration),[53] which scales as $N^{2\upsilon+1}$, with υ being the Flory exponent (0.5 for an ideal chain and 0.588 for a random coil). We do not believe this scaling interpretation is particularly useful for the system considered in this work. First, chain lengths considered only span two orders of magnitude, hardly the length scales relevant for true scaling analysis. Where scaling laws could fit translocation data, i.e., the downhill free energy regime created by strong adsorption potential, the free energy cannot scale with N, as continued pore loading will result in a dramatic increase in free energy. In addition, previous work has found the FP approach[14] to accurately describe forced translocation values in experiment.[49,54]

The results of this MC study are qualitatively similar to previous work where the free energy landscape was calculating using SCFT.[12] Most notably, the prediction of free

energy minima, and the corresponding increase of translocation times, was found using SCFT. One notable difference is our previous work with SCFT did not probe overly strong adsorption potentials, where translocation times of strongly adsorbing systems are faster than the translocation time of the weakly adsorbing systems. While SCFT can make many useful predictions of ideal and excluded volume chains, the real strength of the current approach is the use of a chemically accurate model, which can be upgraded for more complex pore geometries and inhomogeneous polymers, including random and block copolymers. Many factors influence translocation in experiment: temperature, chemical and substrate heterogeneities, solvent composition, hydrodynamic and electrostatic effects, and so on. Many of these variables can be incorporated with relative ease into a molecular simulation. Use of such accurate and realistic potentials may help to resolve the many still open questions about polymer translocation.

The main methodological outcome of this work is the demonstration of the efficiency of the suggested simulation technique (a combination of MC calculation of the free energy landscape by use of the incremental gauge cell method, coupled with application of the FP equation) for modeling translocation dynamics. This technique can be applied not only to adsorption driven translocation, but also to any forced or diffusive translocation process in various confining geometries, including the escape of initially confined chain from a small *cis* compartment to a large *trans* compartment. This is enforced by the fact that two entirely different simulation techniques, SCFT in Ref. 12, and incremental gauge cell MC simulation in this work, bring about similar quantitative conclusions about the specifics of the adsorption-driven translocation is by itself a valuable theoretical result.

Finally, these results suggest an interesting complication to the traditional picture of polymer chromatography. The retention time of a polymer in a column, and thus the quality of chromatographic separation, is found by determining the partition coefficient for a given polymer/solvent and substrate. Traditionally, the partition coefficient is modeled as a function of the difference of free energy upon adsorption from the mobile "free" state to the adsorbed state. When this difference is zero, steric repulsion is balanced by attractive enthalpic interactions, and retention becomes independent of chain length. This condition is called the critical point of adsorption and important in the separation of structured polymers (e.g., functionalized polymers and copolymers).[50] This work suggests that an intermediate state, the partially adsorbed polymer, exist. If adsorption interactions are favorable and the pore imposes a steric penalty as the polymer fills the pore, a metastable partially adsorbed state is reached. This has clear implications in the separation of high weight polymers. We intend to examine this scenario in future work.

ACKNOWLEDGMENTS

The authors thank Dr. Shuang Yang for implementation of the FP equation and for useful discussions. This work was supported by the National Science Foundation (NSF) Chemical, Bioengineering, Environmental, and Transport Systems (CBET) grant "Multiscale Modeling of Adsorption Equilibrium and Dynamics in Polymer Chromatography," NSF Integrative Graduate Education and Research Traineeship (IGERT) program in Nano-Pharmaceutical Engineering, and Venkatarama Fellowship awarded to C.J.R.

[1] M. Muthukumar, *Polymer Translocation* (CRC Press, Boca Raton, FL, 2011).
[2] B. Alberts, A. Johnson, J. Lewis, M. Raff, K. Roberts, and P. Walter, *Molecular Biology of the Cell*, 4th ed. (Garland Science, 2002).
[3] S. Casjens, *Virus Structure and Assembly*, 1st ed. (Jones & Bartlett, 1985).
[4] G. Schatz and B. Dobberstein, Science **271**(5255), 1519 (1996).
[5] A. Meller, J. Phys.: Condens. Matter **15**(17), R581 (2003).
[6] H. W. C. Postma, Nano Lett. **10**(2), 420 (2010).
[7] H. Pasch and B. Trathnigg, *HPLC of Polymers* (Springer-Verlag, Berlin, 1999).
[8] C. A. Merchant, K. Healy, M. Wanunu, V. Ray, N. Peterman, J. Bartel, M. D. Fischbein, K. Venta, Z. Luo, A. T. C. Johnson, and M. Drndić, Nano Lett. **10**(8), 2915 (2010); S. Alapati, D. V. Fernandes, and Y. K. Suh, J. Chem. Phys. **135**(5), 055103 (2011).
[9] M. Bernaschi, S. Melchionna, S. Succi, M. Fyta, and E. Kaxiras, Nano Lett. **8**(4), 1115 (2008).
[10] P. J. Park and W. Sung, J. Chem. Phys. **108**(7), 3013 (1998).
[11] K. Kiran Kumar and K. L. Sebastian, Phys. Rev. E **62**(5), 7536 (2000).
[12] S. Yang and A. V. Neimark, J. Chem. Phys. **136**(21), 214901 (2012).
[13] A. Milchev, K. Binder, and A. Bhattacharya, J. Chem. Phys. **121**(12), 6042 (2004).
[14] M. Muthukumar, J. Chem. Phys. **111**(22), 10371 (1999).
[15] W. Sung and P. J. Park, Phys. Rev. Lett. **77**(4), 783 (1996).
[16] D. K. Lubensky and D. R. Nelson, Biophys. J. **77**(4), 1824 (1999); J. Chuang, Y. Kantor, and M. Kardar, Phys. Rev. E **65**(1), 011802 (2001).
[17] S. Mirigian, Y. Wang, and M. Muthukumar, J. Chem. Phys. **137**(6), 064904 (2012).
[18] C. Y. Kong and M. Muthukumar, J. Chem. Phys. **120**(7), 3460 (2004).
[19] R. Metzler and J. Klafter, Biophys. J. **85**(4), 2776 (2003).
[20] V. V. Lehtola, R. P. Linna, and K. Kaski, Phys. Rev. E **81**(3), 031803 (2010); D. Wei, W. Yang, X. Jin, and Q. Liao, J. Chem. Phys. **126**(20), 204901 (2007); V. V. Lehtola, R. P. Linna, and K. Kaski, Phys. Rev. E **78**(6), 061803 (2008).
[21] P. Tian and G. D. Smith, J. Chem. Phys. **119**(21), 11475 (2003).
[22] J. L. A. Dubbeldam, V. G. Rostiashvili, A. Milchev, and T. A. Vilgis, Phys. Rev. E **83**(1), 011802 (2011).
[23] J. L. A. Dubbeldam, V. G. Rostiashvili, A. Milchev, and T. A. Vilgis, Phys. Rev. E **85**(4), 041801 (2012).
[24] F. Kapahnke, U. Schmidt, D. W. Heermann, and M. Weiss, J. Chem. Phys. **132**(16), 164904 (2010).
[25] S.-S. Chern, A. E. Cárdenas, and R. D. Coalson, J. Chem. Phys. **115**(16), 7772 (2001); J. K. Wolterink, G. T. Barkema, and D. Panja, Phys. Rev. Lett. **96**(20), 208301 (2006).
[26] J. L. A. Dubbeldam, A. Milchev, V. G. Rostiashvili, and T. A. Vilgis, Phys. Rev. E **76**(1), 010801 (2007).
[27] D. B. Wells, V. Abramkina, and A. Aksimentiev, J. Chem. Phys. **127**(12), 125101 (2007).
[28] A. Milchev, J.Phys.: Condens. Matter **23**(10), 103101 (2011).
[29] M. Muthukumar, J. Chem. Phys. **118**(11), 5174 (2003).
[30] P.-G. de Gennes, *Scaling Concepts in Polymer Physics* (Cornell University Press, 1979).
[31] Y. Brun and P. Alden, J. Chromatogr. A **966**(1-2), 25 (2002).
[32] C. J. Rasmussen, A. Vishnyakov, and A. V. Neimark, J. Chem. Phys. **135**(21), 214109 (2011).
[33] A. V. Neimark and A. Vishnyakov, Phys. Rev. E **62**(4), 4611 (2000); A. V. Neimark and A. Vishnyakov, J. Chem. Phys. **122**(23), 234108 (2005).
[34] S. K. Kumar, I. Szleifer, and A. Z. Panagiotopoulos, Phys. Rev. Lett. **66**(22), 2935 (1991).
[35] C. J. Rasmussen, A. Vishnyakov, and A. V. Neimark, Adsorption **17**(1), 265 (2011).
[36] C. J. Rasmussen, A. Vishnyakov, M. Thommes, B. M. Smarsly, F. Kleitz, and A. V. Neimark, Langmuir **26**(12), 10147 (2010).
[37] A. V. Neimark and A. Vishnyakov, J. Phys. Chem. B **109**(12), 5962 (2005); A. V. Neimark and A. Vishnyakov, J. Chem. Phys. **122**(17), 174508 (2005); A. V. Neimark and A. Vishnyakov, *ibid.* **122**(5), 054707 (2005); A. Vishnyakov and A. V. Neimark, *ibid.* **119**(18), 9755 (2003).

[38]A. V. Neimark, P. I. Ravikovitch, and A. Vishnyakov, Phys. Rev. E **65**(3), 031505 (2002); A. V. Neimark and A. Vishnyakov, J. Phys. Chem. B **110**(19), 9403 (2006); A. Vishnyakov and A. V. Neimark, *ibid.* **105**(29), 7009 (2001); A. Vishnyakov and A. V. Neimark, Langmuir **19**(8), 3240 (2003).
[39]P. Kowalczyk, A. Ciach, and A. V. Neimark, Langmuir **24**(13), 6603 (2008).
[40]J. I. Siepmann and D. Frenkel, Mol. Phys. **75**(1), 59 (1992).
[41]H. Flyvbjerg and H. G. Petersen, J. Chem. Phys. **91**(1), 461 (1989).
[42]D. R. Kent, R. P. Muller, A. G. Anderson, W. A. Goddard, and M. T. Feldmann, J. Comput. Chem. **28**(14), 2309 (2007).
[43]J. Gao and J. H. Weiner, J. Chem. Phys. **91**(5), 3168 (1989).
[44]S. K. Kumar, J. Chem. Phys. **96**(2), 1490 (1992).
[45]P. Grassberger and R. Hegger, J. Phys.: Condens. Matter **7**(16), 3089 (1995).
[46]M. S. A. Baksh and R. T. Yang, AIChE J. **37**(6), 923 (1991).
[47]T. Spyriouni, I. G. Economou, and D. N. Theodorou, Macromolecules **30**(16), 4744 (1997); A. V. Neimark, P. I. Ravikovitch, M. Grün, F. Schüth, and K. K. Unger, J. Colloid Interface Sci. **207**(1), 159 (1998).
[48]C. J. Rasmussen, G. Y. Gor, and A. V. Neimark, Langmuir **28**(10), 4702 (2012).
[49]J. Li and D. S. Talaga, J. Phys.: Condens. Matter **22**(45), 454129 (2010).
[50]W. Radke, in *Macromolecular Engineering*, edited by K. Matyjaszewski, Y. Gnanou, and L. Leibler (Wiley-VCH, 2007), p. 1881.
[51]A. Bhattacharya, W. H. Morrison, K. Luo, T. Ala-Nissila, S. C. Ying, A. Milchev, and K. Binder, Eur. Phys. J. E **29**(4), 423 (2009).
[52]O. V. Krasilnikov, C. G. Rodrigues, and S. M. Bezrukov, Phys. Rev. Lett. **97**(1), 018301 (2006).
[53]A. Milchev, J. L. A. Dubbeldam, V. G. Rostiashvili, and T. A. Vilgis, Int. J. Transp. Phenom. **1161**, 95 (2009).
[54]A. J. Storm, J. H. Chen, H. W. Zandbergen, and C. Dekker, Phys. Rev. E **71**(5), 051903 (2005); A. J. Storm, C. Storm, J. Chen, H. Zandbergen, J.-F. Joanny, and C. Dekker, Nano Lett. **5**(7), 1193 (2005).